ISBN: 978-3-95450-132-8 doi:10.18429/JACoW-IPAC2014-WEYB01

LARGE DYNAMIC RANGE BEAM DIAGNOSTICS FOR HIGH AVERAGE CURRENT ELECTRON LINACS

P. Evtushenko[#], JLab, Newport News, USA

Abstract

A number of applications is envisioned now for CW electron LINACs with high average current. A few examples are: driver-accelerators for the next generation of high average brightness SR sources, energy recovery LINACs to be used for frontier research in particle physics - search for dark matter candidate particles, industrial and defense applications. An average beam power of few MW is considered for such applications. Such machines will be required to operate simultaneously with high beam power and peak brightness comparable to the brightest electron beams generated in pulsed LINACs. Combining the high current advantages of storage rings and high peak brightness of LINACs will require such understanding and control of the beam dynamics that 10^{-6} fraction of the beam current or even smaller are taken in to account and controlled during the beam tuning. To make this possible a number of large dynamic range (LDR) beam diagnostics is under development and test at JLab FEL. We describe status of these diagnostics for transverse and longitudinal LDR beam profile measurements, which in turn can be used for LDR measurements of the phase space distribution and its evolution through the accelerator.

MOTIVATION – JLAB FEL EXPERIENCE

It was proposed that LINACs with average current of a mA on the order of magnitude and beam energy in the range 0.6 – 4 GeV can be used as the drivers for next generation of high average brightness light sources operated in X-ray wavelength range in seeded FEL configuration [1-5]. The existing pulsed FELs, operating now in the soft and hard X-ray wavelength ranges, utilize average currents many orders of magnitude less than the above-mentioned mA.

Operation of the IR/UV-Upgrade at Jefferson Lab with average beam current of up to 9 mA and beam power of 1.2 MW has given large experience base with high-current LINAC operation [6]. The primary operational difference between such high current LINACs and storage rings, even with a few hundred mA of average current, is that LINAC beams have neither the time nor a mechanism to come to equilibrium, in contrast to storage ring beams, which are mostly Gaussian. The operational impact of this is significant. When a LINAC is setup, by establishing the longitudinal and transverse match, a diagnostic beam mode with small average current is used. A beam setup is based, most frequently, on measured mean and RMS parameters such as beam size, bunch length, and energy spread. When going from diagnostic mode to higher duty cycle and CW operation, it is frequently found that the "best" RMS-data-based setup must be changed to allow for high current operation to eliminate beam losses. Even when this modification is successful, it is time-consuming process involving some trial and error. It is frequently unclear what the sources of the problem are, and which adjustments to the low-density parts of the phase space distribution were effective in improving performance. This is highly undesirable for any user facility where high availability is required. It is significant that, the resulting setup does not necessarily provide the best beam brightness and is a compromise between acceptable brightness and acceptably low beam losses.

Contributing to this problem is the fact that the measurements used for machine setup are typically based on methods with a dynamic range of 10^3 or even much smaller. Then small, but relevant, low-intensity and large-amplitude parts of the beam phase space distribution are simply not visible during machine tuning.

We have suggested previously that the proper solution to the aforementioned "tune-up problem" is to base the tuning on the measurements with much larger dynamic range such that, the very low intensity and large amplitude parts of phase space distribution are taken in to account. We are presently developing such diagnostics at the JLab. One of the techniques under development is a large dynamic range (LDR) beam imaging. We have previously reported [7] on the increase of the beam imaging dynamic range by a factor of 10^2 from ~ 5×10^2 to about 5×10^4. We have also shown that when applied to non-Gaussian LINAC beams DR of the measurements can significantly impact measured beam parameters such as emittance and Twiss parameters.

In this contribution we report on further development of transverse beam profile measurements, which are targeting dynamic range of at least 10^6.

DIFFRACTION EFFECTS, APODIZATION

In imaging the intensity distribution, measured by imaging sensor, is a convolution of the source distribution and so-called point spread function (PSF). PSF is the distribution on the imaging sensor resulting from a transversely infinitely small source. Diffraction is the main root of PSF, but transmitted wave front errors, due to imperfections of optical elements, can contribute to the PSF as well. PSF is, usually, evaluated in respect to transverse resolution, and optical systems are designed to have the transverse size of the PSF central peak significantly smaller than the object size on the detector. For a LDR imaging application design of a PSF bears additional considerations. Figure 1 helps to demonstrate it. The figure shows a Gaussian distribution, modeling an idealized beam with RMS of the distribution of 25 μm,

*Work supported by US DOE office of Basic Energy Sciences under the early career program; DOE award number FWP#JLAB-BES11-05
Pavel.Evtushenko@jlab.org

ISBN: 978-3-95450-132-8 doi:10.18429/JACoW-IPAC2014-WEYB01

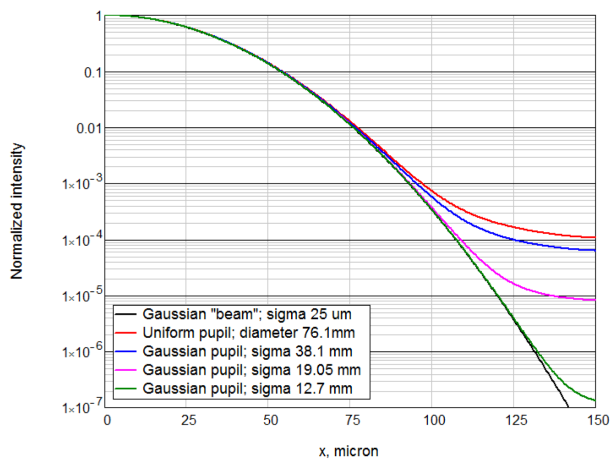

Figure 1: Gaussian distribution compared to its convolutions with PSFs from Figure 2.

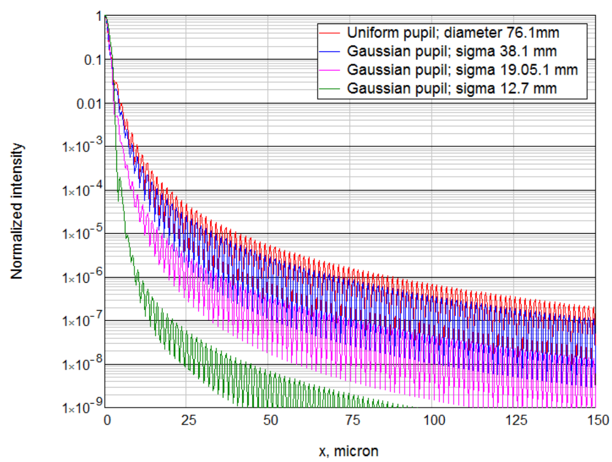

Figure 2: PSFs of uniform and Gaussian pupil functions.

and convolutions of four different PSFs with this Gaussian distribution. The upper most curve corresponds to a PSF of, a typically used, uniformly transparent entrance pupil. It can be easily seen that, the convolution follows the Gaussian distribution well for about two decades, where it starts visible to deviate. When the Gaussian distribution reaches the level of 10^{-4} the deviation is about 300 %, and by the time the Gaussian distribution reaches the level of 10^{-6} the difference is more than two orders of magnitude.

Similar calculations made for the imaging system used in [7], assuming 2D Gaussian beam, show that, within the dynamic range of 5×10^4 and for Gaussian beam with $\sigma_x = \sigma_y > 50\ \mu m$ the measured distributions were not affected by the diffraction "tails" of the PSF. The calculations also show that, dynamic range of 10^6 is, essentially, not achievable in practical optical system, which have to fit in to an accelerator beam line environment. Increasing the solid angle, in which light is collected, in general, improves the dynamic range but does not allow to achieve the 10^6 range. Therefore, some radical changes in the optics are required, if we shall achieve this level of the dynamic range for beam imaging.

To calculate point spread function of an optical system, Fourier optics methods are used. For a practical optical system, used for beam imaging at an accelerator at optical wavelength, Fresnel approximation is valid in general. One of the basic facts of Fourier optics is that, to a very good degree, the distribution in the image plane is a 2D Fourier transform of the lens aperture shape. From this point of view it is easy to understand that, the large-radius low intensity tails of the PSF are due to the sharp step-like edges of the lens pupil function. Indeed, to describe a step function in a frequency domain infinitely large frequencies are required. If the step-like changes of the lens transmission at its edge is the root cause of the large-radius low intensity diffraction tails of the PSF, it is only natural to suggest that elimination of this step-like changes will reduce the intensity of the tails, and might provide the necessary improvement of the PSF. Apodization is a modification of the lens transmission as a function of transverse coordinate within pupil. A number of different apodization approaches have been proposed and investigated numerically, for instance, in astronomy applied to extrasolar planets search. Amplitude of phase of a wave front, transmitted through an apodizer, can be modifier, or a combination of both can be used. There are axis-symmetrical and asymmetrical apodizers considered.

Our requirements to an apodizer are following. Since we need to measure beams profiles of any shape orientation or skew, we require an axis-symmetrical apodizer. Ideally, we would have an achromatic apodizer, since one of the directions that we are investigating is imaging with optical transition radiation (OTR). Another imaging option is to use a thin YAG:Ce scintillators. Although, compared to OTR, YAG:Ce spectrum is relatively narrow, it still spans about 100 nm. We also prefer and apodizer that is easier to manufacture, and the manufacturing technique needs to be accurate and reproducible. We investigate, as a first option, an axis-symmetrical amplitude apodizer, rejecting a phase apodizer mainly for the chromaticity considerations.

We have evaluated numerically several options for the apodization function of the amplitude apodizer. Trying to keep things as simple as possible, we have started considering Gaussian and super-Gaussian dependencies of the transmission.

The evaluation process and criteria are the following. We are considering a simplest imaging system consisting of one effective lens. The apodizer is located in the lens plane, which is also a Fourier plane in respect to the image plane. The magnification of 1/3 and the solid angle, in which light is collected of 2π×115 mrad are chosen close to what we can have in a practical optical system. PSFs are calculated, numerically evaluating the general Huygens integral. An isotropic and monochromatic source with wavelength of 550 nm was assumed. For the evaluation we use, again, a simple 2D Gaussian model of a beam with transverse beam size corresponding to the smallest beam size, which we expect to measure. Convolution of the calculated PSF and the Gaussian beam is computed then, which is done in 2D frequency domain,

ISBN: 978-3-95450-132-8 doi:10.18429/JACoW-IPAC2014-WEYB01

where the convolution is a product. From the convolution we take a cross-section going through its middle and compare that cross-section with the corresponding one of the original Gaussian "beam". An apodization function, which provides larger range, in which the convolution does not deviate significantly from the original distribution, is considered to be the better one. Among the apodization functions, which we have considered a Gaussian apodization have shown better performance. For the first experimental test we have decided to use a Gaussian apodizer with the transmission depending on radius as $T(r) = T_0 \cdot e^{-\left(\frac{r}{\sigma\sqrt{2}}\right)^2}$, with $\sigma = R_{ap}/3$ where R_{ap}- the apodizer radius and T_0 is the transmission in the center, which is close to 100 %.

The described above evaluation process is illustrated in Figs. 1 and 2. Four PSFs are shown in Fig. 2. The four corresponding pupil functions are: uniform - unapodized function with transmission of 100 % at any point on the lens (red), and three Gaussian apodizing functions with σ of R_{ap} (blue), $R_{ap}/2$ (magenta) and $R_{ap}/3$ (green). One can see in the Fig. 2 that the apodization with $\sigma = R_{ap}/3$ reduces the intensity of the large-radius diffraction "tails" by about three orders of magnitude. Figure 1 shows comparison of the original Gaussian distribution and the four convolutions of this Gaussian distribution with the PSFs from Fig.2. There it can be seen that, if the uniform unapodized optics could support dynamic range of less then 10^3, the Gaussian apodization with the $\sigma = R_{ap}/3$ improves the dynamic range to 10^6.

One must add that the improvements of the PSF and the usable dynamic range do not come for free, as a figure of speech. The overall transmission of the optical system is reduced and the transverse resolution is worsen due to the apodization. Although we have paid attention to these effects, they were not a part of the optimization for now, as our main focus and challenge is the dynamic range improvement. However, the transverse resolution of the $\sigma = R_{ap}/3$ apodized system increases only by about 65 %, and remains at the 1 μm level, which is still very small. This is due to rather large numerical aperture of the initial, unapodized imaging system.

APODIZERS

Manufacturing of the required amplitude apodizer is a considerable technological challenge. Scattering and parasitic reflections must be avoided as much as possible in a LDR imaging system, to avoid creation of background sources. This puts additional requirements on the apodizer. Amplitude apodizers can be made based either on a continuously variable partially reflective coating or on a partially absorptive coating. One concern with the partially reflective metal coating of a variable thickness is that optical properties of thin films can be substantially different from those of a bulk material. Also as the coating becomes thinner, at some point, it becomes a non-continuous film and would consist of separate islands. Prediction and control of optical properties under such conditions becomes very difficult. The partially reflective coating would have both a real and imaginary components of the refractive index and therefore would introduce corresponding phase shift, acting as a phase apodizer with not well predictable behavior. Hence, is seems reasonable to assume that a better apodizer should be provided using partially absorptive coatings with constant thickness. However, it is possible that, partially reflective coatings with continuously variable thickness could be more economical to manufacture and still meets the requirements. With this in mind we explore both possibilities in parallel. The process of apodizer manufacturing needs to be accurately controlled and repeatable. Sensitivity study of the apodizer parameters T_0 and σ show that, the deviation of the parameters should not be more than 10 %. Apodizers were manufactured for LDR beam imaging at JLab FEL using two different technologies. One of the approaches uses continuously variable partially reflective coating made via electron beam evaporation of the coating material and a specially designed rotating mask. Another approach is based on so-called "half-tone dot" process. The second apodizer has mostly absorptive coating, which is made of a very large number of microdots with diameter of about 10 μm. In essence, it is a 2D array of 10 μm pixels which have transparency of either 0 or 100 %. Optical density of such a coatings is adjusted through the local density of the microdots. The required optical density profile is converted into the microdot density utilizing "error-diffusion" algorithm [8]. The claim of the error-diffusion algorithm, when it is used for Fourier plane apodizer design, is that the artifacts, arising form the discrete nature of the apodizer, appear only at spatial frequencies higher than a specific one. The size of the pixels is selected then in such a way that, the specific frequency is high enough not to affect, in our case, the beam image. Manufacturing of such apodizers is essentially numerically controlled providing very well controlled process and therefore being more promising.

APODIZER TEST BENCH

With the first prototype apodizers for beam diagnostics at JLab manufactured, we have started their evaluation on an optical test bench. As a source, for first tests, we used back illuminated pinhole. For the initial - preliminary results, presented here, 100 μm diameter pinhole was illuminated by a white LED. In future the LED will be replaced by a narrow band one, with peak wavelength close to the peak of the YAG:Ce emission spectrum at 550 nm. The pinhole is imaged on to a CCD camera by means of two achromatic doublets. In terms of imaging properties, the two doublets can be represented by one effective - imaginary lens, located between the two doublets. The optical setup is designed in such a way that, there is sufficient space between the doublets for the apodizer to be placed in the plane of the effective lens. This is one of key aspects of an apodized optical system, with apodization in a Fourier plane. The apodizer is held

ISBN: 978-3-95450-132-8 doi:10.18429/JACoW-IPAC2014-WEYB01

in place by a spring loaded holder that applies only axial force to the apodizer substrate to minimize the transmitted wave front error. Data presented here were acquired with a single 12-bit CCD. Careful adjustment of the camera black level, measurements and subtraction of background, making the measurements in a light shielded enclosure and averaging over a large number of frames allow for dynamic range of the measurements approaching 12-bit. Due to sharp, step-like edges of the pinhole, one can observe effect of apodization within this dynamic range. The ultimate goal for the bench measurements would be measurements of the apodized optical system PSF.

Figures 3 and 4 show two images of the pinhole recorded without an apodizer and with the Gaussian apodizer. Qualitatively one can easily see that the amount of artificial, diffraction caused halo, around the sharp edge hole is significantly reduced. The only difference in the optical setup between the two pictures was insertion of the apodizer. Quantitatively the apodizer reduces intensity of the diffraction induced tails of the PSF by up to 2×10^3, which is the order of magnitude predicted by modeling.

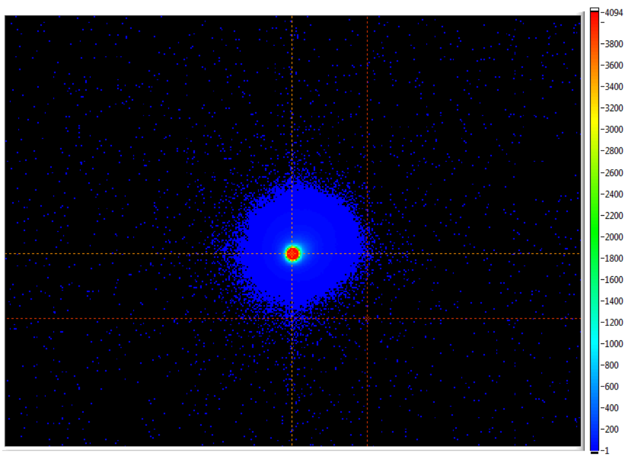

Figure 3: Pinhole image without an apodizer.

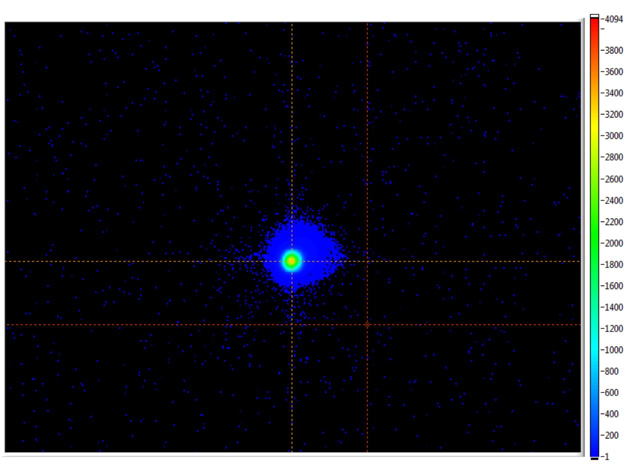

Figure 4: Pinhole image with Gaussian apodizer.

LDR WIRE SCANNER MEASUREMENTS

There is a need for an alternative to imaging based LDR transverse beam profile measurements. There are, at least, two reasons for this. First, since realization of large dynamic range imaging imposes many challenges, it is desirable to have a different technique, which could be used to cross-check the results of the LDR imaging. This would be especially important at the development stage of LDR imaging. Such alternative technique must be based on different underlying physical processes. Mainly, it should not rely on optics and imaging sensors with limited dynamic range. Second and, maybe, more important reason is that at the accelerators, which today provide beams with highest peak brightness, for instance, LCLS, FLASH, beam imaging at the optical wavelength has become either very challenging or impossible. That is attributed to micro-bunching instability, which in a combination with bunch compression leads to a longitudinal modulation of the electron bunch at the wavelengths shorter than the optical one. Overviews of this process from beam diagnostics prospective and its implications to X-ray FEL diagnostics were made recently [9,10]. It is reasonable to assume that, at some of future accelerators with comparable peak beam brightness but average beam current many orders of magnitude higher, this problem will continue to exist. Transverse beam profile measurements with wire-scanners is another well developed technique, which, under certain conditions, was shown to be large dynamic range capable [11]. Thus in parallel to LDR imaging development we are working on LDR wire scanner measurements, which could be made at the same location on the beam line as the LDR imaging. Fig. 5 shows a CAD model of a diagnostics station developed for JLab FEL, which enables such cross-check measurements. Such diagnostic setup contains a beam viewer, a wire-scanner and an impedance shield necessary for high average current CW operation. The beam viewer could be either an OTR or a YAG:Ce viewer or any other thin scintillator, it can be setup either 45 degree or normal relative to the beam direction.

A disadvantage of wire scanner measurements is that, no 2D beam distributions are measured, but only two or three 1D projections of the distribution. This is especially inconvenient for LINAC beams, which do not have Gaussian, i.e., equilibrial distribution and can have rather complicated distribution. Nevertheless, for the cross-check purposes of LDR imaging, a projection of a beam distribution measured with the wire-scanner can be compared with a projection calculated from a 2D beam distribution of the same beam measured by means of LDR imaging. One advantage of wire-scanner measurements is that their detection scheme can be made optics free, i.e., unaffected by the limitation of the dynamic range associated with diffraction. Another advantage is that photo multiplier tubes (PMT) can be used as detectors. As will be described, there are several techniques that allow to measure PMT signal with dynamic range larger than 10^6.

One of a few transverse beam profile measurements made with large dynamic range was made with a wire scanner [11]. CEBAF beam with average current of about 5 nA was measured. The very low average current

ISBN: 978-3-95450-132-8 doi:10.18429/JACoW-IPAC2014-WEYB01

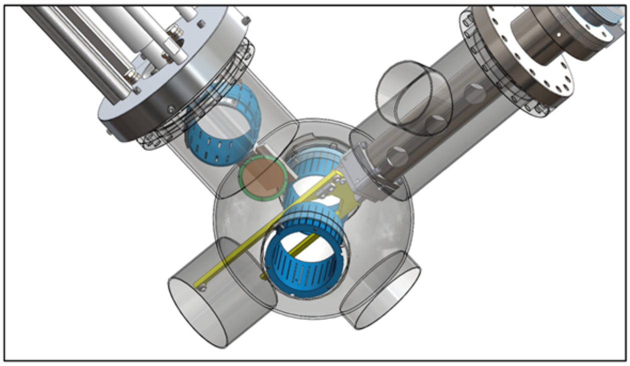

Figure 5: JLab FEL diagnostic module for LDR imaging and wire scanner transverse beam profile measurements with built-in impedance shield

allowed for measurements with CW beam, which had bunch repetition rate of 499 MHz. The key aspect of the measurements that provided the large dynamic range was to use detecting PMTs in photon counting mode. The local beam intensity integrated alone the line of the wire was encoded in to the counting frequency, which can be measured in a very large range. One must note, however, that when photon counting is used, maximum usable frequency is somewhat smaller than the bunch frequency. It is possible to build counting detection system with maximum counting frequency of a couple of hundred MHz. From this prospective wire scanner measurements via photon counting is well suited for accelerators with bunch frequency of few hundred MHz. For measurements presented in [11] the maximum counting frequency was only about 10 MHz, which led to rater long measurements time of single beam profile of about 15 minutes. For LINACs with bunch frequency of about one MHz the dynamic range achievable using photon counting is inevitable smaller, since even for very carefully selected PMTs dark count rate is 10 Hz on the order of magnitude. For such class of accelerators counting would give not only reduced dynamic range but also rather long measurement time. Nevertheless, counting is the easiest way to provide for a linearity in a very large range.

For accelerators with bunch frequency of about MHz, analog mode, i.e., PMT current measurements, can be used to achieve larger dynamic range and to keep measurement time short. Following factors limit dynamic range of a PMT used in analog mode. The average current through a PMT is, most frequently, limited to about 100 µA. However, because a diagnostic beam mode with low duty cycle is used for the measurements, detection system can be setup in such a way that the PMT current during diagnostic mode macro pulse is much higher that the average 100 µA. If one takes CEBAF as an example, where beam mode used for wire scanner measurements is 100 µs long macro pules repeating at 60 Hz, corresponding to 0.6 % duty cycle, the PMT current during the 100 µs long macro pulse can be as high as ~ 16 mA. The dark current, of PMTs specifically made for low dark current, is at the level of a couple of nA, typical, and usually specified to be no more than 20 nA. Thus, in principal, PMT themselves, when carefully selected, are easily suitable for current measurements with the range larger than 10^6. One also should note that, the average current through a PMT with gain of 2×10^6 and used in counting mode at the average count rate of 100 MHz is ~ 32 µA, i.e., 500 times smaller than the 16 mA. This shows that, for small duty cycle beams, counting mode does not allow to exploit the full potential of PMTs it terms of upper limit of the dynamic range. On the other hand, properly selected PMT has dark count rate of 10 Hz on the order of magnitude. For the PMT from the previous example, this corresponds to average current of only 3.2 pA, i.e., about 1000 times smaller than the PMT's smallest dark current. Hence, utilizing counting mode allows for the corresponding dynamic range extension on the low end. Naturally, the largest dynamic range with PMT measurements can be achieved by a combination of analog and counting mode of PMT current measurements and can be on the order of 10^9.

PMT CURRENT MEASUREMENTS

There are several techniques suitable for PMT current measurements with the dynamic range more than 10^6 and in the current range outline above. More detailed description and comparison of these techniques will be presented elsewhere [12]. Here we only briefly mention three most interesting techniques. First, fairly standard one is current-to-frequency conversion, which is in a way related to photon counting. Attractiveness of this technique is in the straightforward way to provide linearity. Another well-known small signal recovery technique for PMT current measurements with very small duty cycle is a combination of gated integrator (GI) and boxcar averager. Our analysis shows that a simple gated integrator can be implemented with the dynamic range of about 10^4. Design of JLab FEL wire-scanner electronics is made with two gated integrators (GI) with dynamic range of 10^4, but with sensitivity different by factor 10^3. This gives an overlap of one order of magnitude in the working range of the two GIs, which is used for their cross-calibration. Output of each GI is digitized by a 16-bit ADC. The measurements of the two GI are combined then in the digital domain in similar way as it is done with 2-CCD camera measurements [7]. Finally, a new and very exiting way to process PMT current in a very large dynamic range is to use logarithmic signal compression by logarithmic detectors originally developed for photo diode current measurements. Such integrated circuits are commercially available and have dynamic range of 120 dB [13] and even 200 dB [14]. Operational range of such logarithmic detectors matches well the above-described PMT current range, 1 nA through 10 mA, which needs to be measured. Notably, these logarithmic detectors have fairly large bandwidth, which is important to keep measurement time short.

ISBN: 978-3-95450-132-8 doi:10.18429/JACoW-IPAC2014-WEYB01

REFERENCES

[1] D. Kraemer et al., “The BESSY Soft X-ray Free Electron Laser”, TDR, ISBN 3-9809534-0-8, BESSY, Berlin

[2] R. A. Bosch et al., “WiFEL: The Wisconsin Free Electron Laser”, Proceedings FEL2009, Liverpool, UK, August 23-28, 2009

[3] S. V. Benson et al., “A proposed VUV oscillator-based FEL upgrade at Jefferson Lab”, Journal of Modern Optics 58 1438 (2011).

[4] J. N. Corlett et al., “Next generation light source R&D and design studies at LBNL”, Proceedings of IPAC12, New Orleans, LA, USA, May 20-25, 2012

[5] J. Galayda, “LCLS-II project”, Proceedings if IPAC14, Dresden, Germany, June 2014

[6] S. V. Benson et al., “Operational aspects of high power energy recovery LINACs”, Proceedings LINAC06, Knoxville, TN, USA, August 21-25, 2006

[7] P. Evtushenko et al., “High Dynamic Range Beam Imaging With Two Simultaneously Sampling CCDs”, Proceedings of FEL2012, Nara, Japan, 2012

[8] C. Dorrer, J. D. Zuegel, “Design and analysis of binary beam shapers using error diffusion,” Journal of the Optical Society of America B Optical Physics 24, 1268–1275 (June 2007)

[9] S. Wesch, “Summary of COTR effects”, Proceedings of DIPAC11, Hamburg Germany

[10] H. Loos, “Beam Instrumentation for X-ray FELs”, Proceedings of DIPAC11, Hamburg Germany

[11] A. P. Freyberger, “Large Dynamic Range Beam Profile Measurements”, DIPAC05, Lion, France

[12] P. Evtushenko et al., “Design of a wire scanner for large dynamic range beam profile measurements” to be published in proceedings of IBIC14

[13] Analog Devices, ADL5303

[14] Analog Devices, ADL5304